HHS Public Access

Author manuscript

Cell Rep. Author manuscript; available in PMC 2016 March 03.

Published in final edited form as:

Cell Rep. 2015 March 3; 10(8): 1252–1260. doi:10.1016/j.celrep.2015.01.060.

Progressive aggregation of alpha-synuclein and selective degeneration of Lewy inclusion-bearing neurons in a mouse model of parkinsonism

Valerie R. Osterberg[1,*], **Kateri J. Spinelli**[1,*], **Leah J. Weston**[1], **Kelvin C. Luk**[2], **Randall L. Woltjer**[3], and **Vivek K. Unni**[1,4,+]

[1]Jungers Center for Neurosciences Research, Oregon Health and Science University, Portland, OR, 97239, USA

[2]Department of Pathology and Laboratory Medicine, Institute on Aging and Center for Neurodegenerative Disease Research, University of Pennsylvania Perelman School of Medicine, Philadelphia, PA, 19104, USA

[3]Department of Pathology, Oregon Health and Science University, Portland, OR, 97239, USA

[4]Parkinson Center of Oregon, Department of Neurology, Oregon Health and Science University, Portland, OR, 97239, USA

Summary

Aggregated alpha-synuclein inclusions are found where cell death occurs in several diseases, including Parkinson's Disease, Dementia with Lewy Bodies and Multiple System Atrophy. However, the relationship between inclusion formation and an individual cell's fate has been difficult to study with conventional techniques. We developed a system that allows for *in vivo* imaging of the same neurons over months. We show that intracerebral injection of preformed fibrils of recombinant alpha-synuclein can seed aggregation of transgenically-expressed and endogenous alpha-synuclein in neurons. Somatic inclusions undergo a stage-like maturation, with progressive compaction coinciding with decreased soluble somatic and nuclear alpha-synuclein. Mature inclusions bear the post-translational hallmarks of human Lewy pathology. Long-term imaging of inclusion-bearing neurons and neighboring neurons without inclusions demonstrates selective degeneration of inclusion-bearing cells. Our results indicate that inclusion formation is

[+]Corresponding author, Correspondence should be addressed to: Vivek K. Unni, Jungers Center & Parkinson Center of Oregon, Oregon Health and Science University, 3181 SW Sam Jackson Park Rd, Mail Code L623, Portland, OR, 97239, USA, unni@ohsu.edu.

[*]These authors contributed equally to this work

Author Contributions:

V.R.O., K.J.S. and V.K.U. designed the study, performed the mouse experiments, interpreted the results and wrote the paper. L.J.W. performed the mouse experiments and interpreted the results. K.C.L provided critical reagents, expertise, interpreted the results and wrote the paper. R.L.W. performed the human pathological experiments, interpreted the results and wrote the paper.

tightly correlated with cellular toxicity and that seeding may be a pathologically relevant mechanism of progressive neurodegeneration in many synucleinopathies.

Introduction

Evidence suggests that many neurodegenerative diseases involve spreading aggregation of specific proteins through the nervous system, potentially via a prion-like mechanism (for review, see Jucker and Walker, 2013, Guo and Lee, 2014, Fraser, 2014). Synucleinopathies are such a group typified by pathologically aggregated alpha-synuclein in specific neuronal (e.g. Parkinon's Disease, Dementia with Lewy Bodies) or glial (e.g. Multiple System Atrophy) populations where cell loss occurs. Recent work demonstrates that aspects of progressive alpha-synuclein aggregation can be recapitulated in model systems by exogenous introduction of *in vitro* generated preformed fibrils (PFFs) of alpha-synuclein (Volpicelli-Daley et al. 2011, Luk et al., 2012a, Luk et al., 2012b, Masuda-Suzukake et al., 2013, Sacino et al., 2014a, Sacino et al., 2014b, Sacino et al. 2014c). PFFs seed the aggregation of endogenous alpha-synuclein and this aggregation spreads along synaptically connected pathways (Luk et al., 2012a, Luk et al., 2012b). One hypothesis is that this seeding involves a prion-like mechanism where introduced PFFs directly convert endogenous alpha-synuclein into an aggregated form that then propagates through the brain. However, recent work questions the ability of PFFs to cause widespread seeding of endogenous alpha-synuclein (Sacino et al., 2014a) and other potential mechanisms for spreading have been proposed (for review, see Brundin et al. 2008, Golde et al., 2013). In addition, the role inclusion development plays in a cell's ultimate fate has been difficult to determine using current techniques. Evidence supporting either an association between Lewy pathology development and compromised cell health (Lu et al. 2005, Greffard et al. 2010) or the opposite, relative neuroprotection (Gertz et al. 1994, Bodner et al. 2006, Tanaka et al. 2004), has been suggested.

To test these mechanisms *in vivo*, we developed a multiphoton imaging approach to monitor conversion of endogenous alpha-synuclein into pathologically aggregated states in living mouse brain after PFF injection. Transgenic mice expressing Green Fluorescent Protein (GFP)-tagged wild-type (WT) human alpha-synuclein (Syn-GFP; Rockenstein et al. 2005) were injected with mouse sequence PFFs in primary sensory cortex and neuronal aggregation of Syn-GFP monitored *in vivo* using multiphoton microscopy. Serial imaging of individual mice allowed us to determine the time course and pattern of inclusion development up to 13 months after PFF injection. *In vivo* multiphoton Fluorescence Recovery After Photobleaching (FRAP) experiments allowed us to measure alpha-synuclein mobility in different somatic pools and detected a slow alpha-synuclein turnover rate within inclusions. These data suggest that exogenously introduced PFFs convert endogenous alpha-synuclein into an aggregated state structurally similar to inclusions found in human disease. Our data further suggest that aggregation is a stage-like process, with progressive compaction and coincident reduction in soluble cytoplasmic and nuclear levels as inclusions mature. Imaging of individual neurons over months detected selective cell death of inclusion-bearing neurons, suggesting a critical role of Lewy pathology in a cell's fate.

Results

In vivo imaging demonstrates a stage-like, progressive maturation of Syn-GFP inclusions within neurons

PFFs were injected into right hemisphere sensory cortex of mice expressing Syn-GFP under control of the PDGF promoter. We placed cranial windows starting at 2 months post-injection (mpi). At this time point the Syn-GFP expression pattern in neuronal cell bodies and presynaptic terminals in PFF-injected animals was unchanged from uninjected or phosphate-buffered saline (PBS)-injected controls (Fig. 1A). Our previous work demonstrated that somatic Syn-GFP is not aggregated, does not spontaneously form inclusions and is freely diffusible in the absence of PFF injection (Unni et al., 2010, Spinelli et al., 2014). Starting at ~2.5 mpi, Syn-GFP aggregates were readily apparent in neurites near the injection site and rarely in the contralateral hemisphere of PFF-injected mice (Fig. 1B). At ~3 mpi, individual neurons near the injection site exhibited heterogeneous somatic Syn-GFP staining, with parts of the same cell body containing normal homogenous staining and other parts abnormal Syn-GFP accumulations (Fig. 1B). At ~4–13 mpi, somatic inclusions increased in frequency near the injection site and took on a morphologically distinct character. Mature inclusions often presented as a cytoplasmic Syn-GFP accumulation (“body”) with tendrils (“legs”) that wrapped around the nucleus, giving mature inclusions a “spider-like” appearance (Fig. 1B). Interestingly, unlike immature inclusions, at this later stage there was a decrease in the normal appearing soluble Syn-GFP staining in the cytoplasm and nucleus, compared to earlier time points (Fig. 1B). Starting at ~4 mpi, mature inclusions were abundant in the contralateral left hemisphere as well (Fig. 1B). Quantitative analysis of Syn-GFP homogeneity across cell bodies demonstrated a single population with low inhomogeneity in all neurons from uninjected and PBS-injected mice (Fig. 1C). In contrast, PFF-injected mice at >3 mpi showed two distinct populations, one with low inhomogeneity (0.11±0.03 inhomogeneity index, N=56 cells/6 animals; Fig 1C) nearly identical to PBS-injected mice (0.10±0.03 inhomogeneity index, N=69 cells/2 animals, one-way ANOVA, $p<0.0001$, Tukey post-hoc testing no significant difference for this comparison; Fig. 1C) and a second population with a significantly higher inhomogeneity (0.47±0.16, N=108 cells/7 animals, Tukey post-hoc test $p<0.05$, Fig. 1C), corresponding to neurons with spider-like inclusions (Fig. 1C).

In vivo multiphoton FRAP demonstrates progressive compaction of Syn-GFP aggregates

Multiphoton FRAP can be used to measure Syn-GFP mobility of distinct pools in different subcellular compartments *in vivo* (Unni et al., 2010, Spinelli et al., 2014). We used this technique to first measure the somatic immobile Syn-GFP fraction in PBS-injected animals. All neurons demonstrated a low somatic immobile fraction (11±7%, N=7 cells/2 animals; Fig. 2C), consistent with our previous work using *in vivo* multiphoton FRAP, Proteinase K digestion and immunohistochemistry demonstrating no spontaneous somatic aggregation (Spinelli et al., 2014). We next performed FRAP on immature inclusions at ~3 mpi. Unlike in somata without aggregated Syn-GFP (in PBS-injected controls), we detected a large immobile fraction measured at 5 minutes post-bleach (70±16%, N=8 cells/3 animals; Fig 2A&C) that was significantly different than somata without inclusions (one-way ANOVA, $p<0.0001$, Tukey post-hoc test $p<0.05$; Fig. 2C). In addition, simultaneous bleaching of

aggregated and unaggregated regions in a single neuron demonstrated an immobile fraction only in the aggregated region of the soma (Fig. 2A). Similar FRAP experiments performed in mature inclusions at ~4–13 months post-injection demonstrated an even larger immobile fraction (97±6%, N=16 cells/4 animals; Fig. 2A&C), significantly different than both unaggregated regions and immature inclusions (one-way ANOVA, $p<0.0001$, Tukey post-hoc test $p<0.05$ for both comparisons; Fig. 2C).

Chronic *in vivo* imaging demonstrates a low molecular turnover rate within aggregates

We extended the time scale of our FRAP experiments to determine if the fraction of Syn-GFP that is immobile on the minutes time scale recovers over longer time scales. These results demonstrated that a partial Syn-GFP fluorescence recovery within the bleached region does occur over 7 days (immobile fraction 5 min: 97±6%, N=16 cells/4 animals; immobile fraction 7 day: 49±17%, N=10 cells/3 animals; one-way ANOVA, $p<0.0001$, Tukey post-hoc test $p<0.05$; Fig 2A–C), corresponding to a 49% decrease in the previously immobile fraction. This indicates that there is a slow turnover of Syn-GFP within inclusions and that unbleached protein, either newly synthesized or from unbleached regions, moves into the bleached region and becomes incorporated over the course of several days.

Mature somatic inclusions bear the hallmarks of human Lewy pathology

Mice were sacrificed and brains fixed for immunohistochemistry at multiple time points following PFF injection. Starting at ~1 mpi, we detected abnormal Syn-GFP accumulations in cortical neuron cell bodies in the right (injected) hemisphere and neurites with an axonal appearance in cortical layers (V/VI), deeper than we can image *in vivo*, while similar accumulations were not seen in the cortex of PBS-injected or uninjected controls (data not shown), consistent with our *in vivo* imaging results (Fig. 1) and our previous work (Spinelli et al. 2014). Starting at ~3 mpi, numerous inclusions were detectible (Fig. 3) in more superficial layers (II/III), with the same mature, spider-like appearance imaged *in vivo* from these same cortical layers (Fig. 1). These inclusions bore all the hallmarks of human Lewy pathology, including significant alpha-synuclein phosphorylation at serine-129 (Fig. $3A_{1–4}$ & $B_{1–2}$), amyloid dye binding (Thioflavin S & X-34, Fig $3A_{1–2}$), and ubiquitination (Fig. $3A_3$). Importantly, numerous similar inclusions composed only of untagged endogenous mouse alpha-synuclein with the same morphology and staining characteristics (Fig. $3A_5$) were found in nearby Syn-GFP-negative cells, strongly suggesting that the GFP tag does not interfere with the mechanism of Lewy pathology formation. Staining with an anti-GFP antibody demonstrated that the green fluorescent inclusions were made of Syn-GFP and not an endogenous, green autofluorescent species or autofluorescence from the injected material itself (Fig. $3A_4$ & B_1). Further evidence for this came from PFF injections in non-transgenic animals, which did not exhibit any green fluorescent inclusions (Fig. S1), also demonstrating that the Lewy pathology we image *in vivo* and in fixed tissue is composed of Syn-GFP and not autofluorescent species. Quantification of Syn-GFP levels within inclusions versus neighboring Syn-GFP-positive neurons without inclusions demonstrated a significant, large increase in Syn-GFP protein within mature Lewy inclusions (17±11 fold increase, N=25 cell pairs/3 animals; $p<0.0001$, paired t-test; Fig 3B). Syn-GFP within inclusions was also significantly more colocalized with phospho-synuclein forms than Syn-GFP in cells without inclusions (average Pearson's coefficient within inclusions: 0.66±0.19, N=22 cells/3

animals; without inclusions: 0.03±0.02, N=22 cells, 3 animals; p<0.0001, t-test; Fig. 3B). Sagittal sections of the injected right hemisphere also demonstrated the presence of cortical and hippocampal inclusions, composed either of Syn-GFP or endogenous mouse alpha-synuclein, at and distant to the injection site along the anterior-posterior axis of the cortex (Fig. S2).

Aggregated cortical alpha-synuclein pathology in human Dementia with Lewy Bodies cases is structurally similar to mature mouse aggregates imaged *in vivo*

Review of alpha-synuclein inclusion pathology stained for serine-129 phospho-forms in frontal cortex in three cases of Dementia with Lewy Bodies revealed numerous somatic inclusions that wrapped around the nucleus with a similar morphology to what we observe with our Syn-GFP inclusions *in vivo* (Fig. $3C_{1–2}$). No staining was seen in a review three age-matched control cases without clinical evidence of dementia (data not shown). In addition, frequent cortical inclusions were found with tendrils of aggregated alpha-synuclein wrapping around the nucleus (Fig. $3C_{3–4}$), again similar to our mature Syn-GFP inclusions in mice.

Selective degeneration of inclusion-bearing neurons

Serial imaging of individual inclusion-bearing and non-inclusion-bearing neurons over the course of 7 months detected a high rate of disappearance of mature Lewy inclusion-bearing cells (40.3% survival at 207 days, N=154 cells/4 animals, Fig. 4A–D). In contrast, adjacent neurons without inclusions had a very low rate of disappearance (99.4% survival at 207 days, N=272 cells/4 animals, Fig. 4A,B&E). This is similar to our previous work demonstrating an undetectable rate of loss of Syn-GFP-expressing neurons (100% survival of 42 cells) in uninjected animals over 49 days (Unni et al., 2010). Survival analysis showed that the presence of mature inclusions was strongly correlated with cell death in the bearing neurons, with a median survival of 113 days (p<0.0001, Mantel-Cox test, Fig. 4F). In addition, we did not detect large-scale changes in the shape of inclusions, even if they persisted for several months (Fig. 4D).

Discussion

We have shown that the intracortical injection of mouse WT alpha-synuclein PFFs into mice expressing human WT alpha-synuclein tagged with GFP leads to the conversion of the transgenically expressed protein into neuritic and somatic inclusions that bear the hallmarks of human Lewy pathology. Previous work has questioned whether PFFs can seed widespread conversion of alpha-synuclein into an aggregated form when it does not contain the A53T point mutation (Sacino et al., 2014a). Specifically, cross-reactivity between phospho-serine-129 synuclein antibodies and neurofilament-L was suggested as the source of signal interpreted as alpha-synuclein aggregates in other experiments. In this work (Sacino et al., 2014a), alpha-synuclein aggregates were only seen distant from injection site in animals expressing the A53T point mutant, although more recent work from the same group does show some evidence of spreading human WT alpha-synuclein aggregation (Sacino et al., 2014c). Our work uses a parallel approach to detect aggregated alpha-synuclein based on endogenous GFP fluorescence. Both in fixed tissue and with *in vivo*

multiphoton imaging, we detect a time-dependent, progressive aggregation of WT human Syn-GFP only after PFF injection and not in controls. In addition, injections localized to sensory cortex in one hemisphere produced a clear spread of aggregation to the contralateral sensory cortex ~3–4 months post-injection. These results, taken together with previous work (Luk et al., 2012a, Luk et al., 2012b, Masuda-Suzukake et al., 2013), suggest that PFFs can seed progressive aggregation of endogenous protein within brain that is not an artifact of antibody cross-reactivity.

Our work is the first, to our knowledge, to examine formation of alpha-synuclein inclusions *in vivo* within neurons individual animals over time. This chronic imaging demonstrates that inclusions undergo a stage-like maturation from early aggregates with disordered morphology alongside normal soluble somatic and nuclear Syn-GFP. Over the course of weeks, however, inclusions change to become organized and compacted into mature forms that resemble human cortical pathology in Dementia with Lewy Bodies. Previous work from cross-sectional studies of human tissue has demonstrated various forms of somatic inclusions that appear less compact than classical Lewy bodies, such as cloud-like inclusions and pale bodies (Dale et al., 1992, Gomez-Tortosa et al., 2000). Several groups have postulated that individual aggregates could undergo progressive compaction along a pathway from diffuse aggregates to more compact Lewy bodies (Dale et al., 1992, Gomez-Tortosa et al., 2000, Wakabayashi et al. 2013). Alternatively, these structures could reflect distinct parallel pathways (Dale et al., 1992). Our work confirms that inclusion maturation can occur *in vivo*, with progressive compaction as measured by FRAP. It will be important in the future to determine what mechanisms underlie this process.

In parallel with inclusion maturation, we measured a reduction in soluble cytoplasmic and nuclear Syn-GFP *in vivo*. It is interesting to speculate about the significance of this reduction, since although a nuclear role for synucleins has been suggested since their initial discovery (Maroteaux et al., 1998), it is less well understood. Specific activities involving intranuclear alpha-synuclein have been recently proposed, however (Desplats et al., 2011, Liu et al., 2011, Ma et al., 2014). It may be that loss of nuclear alpha-synuclein when inclusions mature contributes to cellular dysfunction through a loss-of-function mechanism. This would be in parallel to the better-established toxic, gain-of-function consequences of alpha-synuclein aggregation.

Our work strongly suggests that inclusion-bearing neurons selectively degenerate over the course of months, while non-inclusion-bearing neurons that express soluble Syn-GFP have a much lower rate of degeneration. This addresses a critical question in the field about the relationship between Lewy pathology formation in individual neurons and their ultimate fate. Although it is clear that Lewy pathology is found in regions where progressive cell death occurs (Fearnley & Lees 1991, Parkkinen et al. 2011, Fig. 4G), different models have been proposed (Fig. 4H), including ones where Lewy pathology is associated with death of the containing cell (Lu et al. 2005, Greffard et al. 2010), or the opposite, where Lewy pathology is associated with sparing of cell (Gertz et al. 1994, Bodner et al. 2006, Tanaka et al. 2004). Our work suggests that the former model is correct, and that Lewy pathology formation is strongly associated with degeneration of the inclusion-bearing cell and not protection (Fig. 4H). This argues that Lewy pathology formation itself could play an

intimate role in neuronal cell loss, but more work is needed to test this hypothesis, including methods to selectively label the subgroup of neurons that take up PFFs. This could be used to determine what fraction of neurons that take up PFFs go on to form Lewy pathology. Then, by manipulating Lewy pathology to increase or decrease its formation, it should be possible to test whether the statistical association that we have measured for the first time *in vivo* is due to a causal role for Lewy pathology in cell death, or if more complicated mechanisms are at play and inclusion formation is actually protective, or simply neutral. The injection of other forms of alpha-synuclein (e.g. monomeric and non-fibrillar aggregates) and other amyloidogenic proteins (e.g. tau and beta-amyloid) to test their ability to seed Lewy pathology formation is also of interest for future work in this system, where potential cross-seeding can be studied in individual neurons *in vivo*.

Overall, our work demonstrates that PFFs can seed progressive conversion of endogenous alpha-synuclein into neuronal inclusions that bear the hallmarks of human disease and lead to selective neuronal degeneration. This system provides a new, *in vivo* model for testing mechanisms of alpha-synuclein inclusion formation, neuronal cell loss, and potential pathways to halt neurodegeneration in clinically important synucleinopathies.

Experimental Procedures

Animals

Syn-GFP (PDNG78; Rockenstein et al., 2005) heterozygous male mice were mated to BDF1 females (Charles River) and housed by OHSU's DCM. Animals were held in a light-dark cycle, temperature- and humidity-controlled vivarium and maintained under *ad libitum* food and water diet. All experiments were approved by the OHSU IACUC and every effort was made to minimize the number of animals used and their suffering.

Humans

Human subjects were seen in the Oregon Alzheimer’s Disease Center (ADC) and affected subjects had established clinical diagnosis of dementia. Brain autopsy from three patients diagnosed with Dementia with Lewy Bodies between the ages of 68–79 years and three age-matched control cases without clinical evidence of neurodegenerative disease was performed in the ADC neuropathology core. Tissue use was approved by the IRB at OHSU.

Intracerebral injections & immunohistochemistry

2–3 month-old Syn-GFP mice were injected with mouse WT sequence PFFs, with PBS, or were uninjected controls. Injections were done according to published protocols for PFF generation and preparation (Luk et al., 2012b) and sensory cortex injections (Kuchibhotla et al., 2008). Briefly, 2.5 μL (2mg/mL) freshly sonicated PFFs or 2.5 μL PBS was injected into right hemisphere primary sensory in isoflurane (1–2%) anesthetized animals. For IHC studies, whole brains were dissected and the cerebellum removed. Brains were prepared and imaged using published protocols (Spinelli et al. 2014). Briefly, hemispheres were placed in scintillation vials with 4% paraformaldehyde and fixed using a BioWave (Pelco) microwave fixation system. Hemispheres were postfixed in 4% paraformaldehyde overnight at 4°C and then stored in PBS containing sodium azide (0.05%) until use. pSer129 aSyn (81A, 1:667

dilution; Waxman and Giasson, 2008), ubiquitin (Z0458, 1:200 dilution; Dako), and GFP (AB6556, 1:500 dilution; Abcam) primary antibodies were diluted in blocking buffer and slices incubated overnight at 4°C. Appropriate secondary antibodies (Alexa Fluor 647, Alex Fluor 555; 1:1000; Invitrogen) were incubated overnight at 4°C. Thioflavin S and X-34 staining was performed using standard techniques (Styren et al. 2000). Brain slices were mounted in CFM-2 (Ted Pella), sealed with CoverGrip (Biotium), and allowed to dry overnight in the dark. For confocal imaging, sections were imaged on a Zeiss LSM710 confocal microscope with a Plan-Apochromat 63×/1.40 oil objective. Fluorescence images were analyzed in Fiji (Schindelin et al., 2012) or ImageJ (NIH) with only linear scaling of pixel values. Human neuropathological analysis was done using standard hematoxylin methods. Standard IHC methods were used to evaluate serine-129-phosphorylated alpha-synuclein. In brief, formalin-fixed, paraffin-embedded sections of frontal cortex were incubated with antibody EP1536Y (1:10,000, Abcam), developed with diaminobenzidine chromagen, and counterstained with hematoxalin, as previously described (Leverenz et al., 2008).

Cranial window surgery & imaging

Starting at 2 mpi cranial window surgery was performed and *in vivo* imaging and photobleaching begun similar to published protocols (Spinelli et al., 2014). Isoflurane-anesthetized animals were placed in a custom-built stereotaxic frame and surgery performed to create a ~5-mm-diameter midline circular craniotomy between bregma and lambda, closed with 8 mm coverglass, and a custom-built aluminum fixation bar cemented into place. On imaging days, isoflurane-anesthetized animals were mounted into the stereotaxic frame and imaged using a Zeiss LSM 7MP multiphoton microscope outfitted with dual channel BiG (binary GaAsP) detectors and a Coherent Technologies Chameleon titanium-sapphire femtosecond pulsed laser source (tuned to 860 nm). Zeiss Zen 2011 image acquisition software was used.

Imaging analysis

Images were analyzed with ImageJ or Fiji (Schindelin et al., 2012) as previously described (Spinelli et al., 2014). Briefly, regions of interest (ROIs) were selected to obtain mean fluorescence values in relevant ROIs. The inhomogeneity index was calculated as the average root-mean-square deviation of the normalized fluorescence signal across a transect of the cell body. FRAP data were analyzed in Prism 5 (GraphPad) to obtain single exponential fits to the recovery time course, the immobile, and mobile fractions. For chronic inclusion imaging >1 day, individual bleached ROI intensities were normalized to unbleached regions to control for possible differences in imaging conditions present on different days.

Statistics

All data are reported as the mean ± SD. Numbers and statistical tests used are reported in relevant sections.

Supplementary Material

Refer to Web version on PubMed Central for supplementary material.

Acknowledgments

We thank Jonathan Taylor for help with mouse colony management, Douglas Zeppenfeld & Jeffrey Iliff for technical assistance with injections, Edward Rockenstein & Eliezer Masliah for Syn-GFP mice, William Klunk for the gift of X-34, Virginia Lee, John Trojanowski & Gary Westbrook for helpful discussions, and Tamily Weissman for helpful discussions and assistance with figure generation. This work was supported in part by the National Institutes of Health (Grants NS069625, AG024978, AT002688, AG008017 and NS061800) and the Pacific Northwest Parkinson's Group.

References

Anderson JP, Walker DE, Goldstein JM, de Laat R, Banducci K, Caccavello RJ, Barbour R, Huang J, Kling K, Lee M, Diep L, Keim PS, Shen X, Chataway T, Schlossmacher MG, Seubert P, Schenk D, Sinha S, Gai WP, Chilcote TJ. Phosphorylation of Ser-129 is the dominant pathological modification of alpha-synuclein in familial and sporadic Lewy body disease. J Biol Chem. 2006 Oct 6; 281(40):29739–29752. Epub 2006 Jul 17. PubMed PMID: 16847063. [PubMed: 16847063]

Bodner RA, Outeiro TF, Altmann S, Maxwell MM, Cho SH, Hyman BT, McLean PJ, Young AB, Housman DE, Kazantsev AG. Pharmacological promotion of inclusion formation: a therapeutic approach for Huntington's and Parkinson's diseases. Proc Natl Acad Sci U S A. 2006 Mar 14; 103(11):4246–4251. Epub 2006 Mar 6. PubMed PMID: 16537516; PubMed Central PMCID: PMC1449678. [PubMed: 16537516]

Brundin P, Li JY, Holton JL, Lindvall O, Revesz T. Research in motion: the enigma of Parkinson's disease pathology spread. Nat Rev Neurosci. 2008 Oct; 9(10):741–745. Epub 2008 Sep 4. Review. PubMed PMID: 18769444. [PubMed: 18769444]

Dale GE, Probst A, Luthert P, Martin J, Anderton BH, Leigh PN. Relationships between Lewy bodies and pale bodies in Parkinson's disease. Acta Neuropathol. 1992; 83(5):525–529. PubMed PMID: 1320323. [PubMed: 1320323]

Desplats P, Spencer B, Coffee E, Patel P, Michael S, Patrick C, Adame A, Rockenstein E, Masliah E. Alphasynuclein sequesters Dnmt1 from the nucleus: a novel mechanism for epigenetic alterations in Lewy body diseases. J Biol Chem. 2011 Mar 18; 286(11):9031–9037. Epub 2011 Feb 4. PubMed PMID: 21296890; PubMed Central PMCID: PMC3059002. [PubMed: 21296890]

Fearnley JM, Lees AJ. Ageing and Parkinson's disease: substantia nigra vregional selectivity. Brain. 1991 Oct; 114(Pt 5):2283–2301. PubMed PMID: 1933245. [PubMed: 1933245]

Fraser PE. Prions and prion-like proteins. J Biol Chem. 2014 Jul 18; 289(29):19839–19840. Epub 2014 May 23. Review. PubMed PMID: 24860092; PubMed Central PMCID: PMC4106303. [PubMed: 24860092]

Fujiwara H, Hasegawa M, Dohmae N, Kawashima A, Masliah E, Goldberg MS, Shen J, Takio K, Iwatsubo T. alpha-Synuclein is phosphorylated in synucleinopathy lesions. Nat Cell Biol. 2002 Feb; 4(2):160–164. PubMed PMID: 11813001. [PubMed: 11813001]

Gertz HJ, Siegers A, Kuchinke J. Stability of cell size and nucleolar size in Lewy body containing neurons of substantia nigra in Parkinson's disease. Brain Res. 1994 Feb 21; 637(1–2):339–341. PubMed PMID: 8180816. [PubMed: 8180816]

Golde TE, Borchelt DR, Giasson BI, Lewis J. Thinking laterally about neurodegenerative proteinopathies. J Clin Invest. 2013 May 1; 123(5):1847–1855. Epub 2013 May 1. PubMed PMID: 23635781; PubMed Central PMCID: PMC3635732. [PubMed: 23635781]

Greffard S, Verny M, Bonnet AM, Seilhean D, Hauw JJ, Duyckaerts C. A stable proportion of Lewy body bearing neurons in the substantia nigra suggests a model in which the Lewy body causes neuronal death. Neurobiol Aging. 2010 Jan; 31(1):99–103. Epub 2008 May 23. PubMed PMID: 18457903. [PubMed: 18457903]

Guo JL, Lee VM. Cell-to-cell transmission of pathogenic proteins in neurodegenerative diseases. Nat Med. 2014 Feb; 20(2):130–138. Review. PubMed PMID: 24504409; PubMed Central PMCID: PMC4011661. [PubMed: 24504409]

Gómez-Tortosa E, Newell K, Irizarry MC, Sanders JL, Hyman BT. alpha-Synuclein immunoreactivity in dementia with Lewy bodies: morphological staging and comparison with ubiquitin immunostaining. Acta Neuropathol. 2000 Apr; 99(4):352–357. PubMed PMID: 10787032. [PubMed: 10787032]

Jucker M, Walker LC. Self-propagation of pathogenic protein aggregates in neurodegenerative diseases. Nature. 2013 Sep 5; 501(7465):45–51. Review. PubMed PMID: 24005412; PubMed Central PMCID: PMC3963807. [PubMed: 24005412]

Kuchibhotla KV, Goldman ST, Lattarulo CR, Wu HY, Hyman BT, Bacskai BJ. Abeta plaques lead to aberrant regulation of calcium homeostasis in vivo resulting in structural and functional disruption of neuronal networks. Neuron. 2008 Jul 31; 59(2):214–225. PubMed PMID: 18667150; PubMed Central PMCID: PMC2578820. [PubMed: 18667150]

Liu X, Lee YJ, Liou LC, Ren Q, Zhang Z, Wang S, Witt SN. Alpha-synuclein functions in the nucleus to protect against hydroxyurea-induced replication stress in yeast. Hum Mol Genet. 2011 Sep 1; 20(17):3401–3414. Epub 2011 Jun 3. PubMed PMID: 21642386; PubMed Central PMCID: PMC3153305. [PubMed: 21642386]

Lu L, Neff F, Alvarez-Fischer D, Henze C, Xie Y, Oertel WH, Schlegel J, Hartmann A. Gene expression profiling of Lewy body-bearing neurons in Parkinson's disease. Exp Neurol. 2005 Sep; 195(1):27–39. PubMed PMID: 15944136. [PubMed: 15944136]

Luk KC, Kehm V, Carroll J, Zhang B, O'Brien P, Trojanowski JQ, Lee VM. Pathological α-synuclein transmission initiates Parkinson-like neurodegeneration in nontransgenic mice. Science. 2012 Nov 16; 338(6109):949–953. PubMed PMID: 23161999; PubMed Central PMCID: PMC3552321. [PubMed: 23161999]

Luk KC, Kehm VM, Zhang B, O'Brien P, Trojanowski JQ, Lee VM. Intracerebral inoculation of pathological α-synuclein initiates a rapidly progressive neurodegenerative α-synucleinopathy in mice. J Exp Med. 2012 May 7; 209(5):975–986. Epub 2012 Apr 16. PubMed PMID: 22508839; PubMed Central PMCID: PMC3348112. [PubMed: 22508839]

Ma KL, Song LK, Yuan YH, Zhang Y, Yang JL, Zhu P, Chen NH. α-Synuclein is prone to interaction with the GC-box-like sequence in vitro. Cell Mol Neurobiol. 2014 May; 34(4):603–609. PubMed PMID: 24659023. [PubMed: 24659023]

Maroteaux L, Campanelli JT, Scheller RH. Synuclein: a neuron-specific protein localized to the nucleus and presynaptic nerve terminal. J Neurosci. 1988 Aug; 8(8):2804–2815. PubMed PMID: 3411354. [PubMed: 3411354]

Masuda-Suzukake M, Nonaka T, Hosokawa M, Oikawa T, Arai T, Akiyama H, Mann DM, Hasegawa M. Prion-like spreading of pathological α-synuclein in brain. Brain. 2013 Apr; 136(Pt 4):1128–1138. Epub 2013 Mar 6. PubMed PMID: 23466394; PubMed Central PMCID: PMC3613715. [PubMed: 23466394]

Parkkinen L, O'Sullivan SS, Collins C, Petrie A, Holton JL, Revesz T, Lees AJ. Disentangling the relationship between lewy bodies and nigral neuronal loss in Parkinson's disease. J Parkinsons Dis. 2011; 1(3):277–286. PubMed PMID: 23939308; PubMed Central PMCID: PMC4196643. [PubMed: 23939308]

Rockenstein E, Schwach G, Ingolic E, Adame A, Crews L, Mante M, Pfragner R, Schreiner E, Windisch M, Masliah E. Lysosomal pathology associated with alpha-synuclein accumulation in transgenic models using an eGFP fusion protein. J Neurosci Res. 2005 Apr 15; 80(2):247–259. PubMed PMID: 15765523. [PubMed: 15765523]

Sacino AN, Brooks M, Thomas MA, McKinney AB, McGarvey NH, Rutherford NJ, Ceballos-Diaz C, Robertson J, Golde TE, Giasson BI. Amyloidogenic α-synuclein seeds do not invariably induce rapid, widespread pathology in mice. Acta Neuropathol. 2014 May; 127(5):645–665. PubMed PMID: 24659240. [PubMed: 24659240]

Sacino AN, Brooks M, Thomas MA, McKinney AB, Lee S, Regenhardt RW, McGarvey NH, Ayers JI, Notterpek L, Borchelt DR, Golde TE, Giasson BI. Intramuscular injection of α-synuclein induces CNS α-synuclein pathology and a rapid-onset motor phenotype in transgenic mice. Proc Natl Acad

Sci U S A. 2014 Jul 22; 111(29):10732–10737. Epub 2014 Jul 7. PubMed PMID: 25002524; PubMed Central PMCID: PMC4115570. [PubMed: 25002524]

Sacino AN, Brooks M, McKinney AB, Thomas MA, Shaw G, Golde TE, Giasson BI. Brain injection of α- synuclein induces multiple proteinopathies, gliosis, and a neuronal injury marker. J Neurosci. 2014 Sep 10; 34(37):12368–12378. PubMed PMID: 25209277. [PubMed: 25209277]

Schindelin J, Arganda-Carreras I, Frise E, Kaynig V, Longair M, Pietzsch T, Preibisch S, Rueden C, Saalfeld S, Schmid B, Tinevez JY, White DJ, Hartenstein V, Eliceiri K, Tomancak P, Cardona A. Fiji: an open-source platform for biological-image analysis. Nat Methods. 2012 Jun 28; 9(7):676–682. PubMed PMID: 22743772; PubMed Central PMCID: PMC3855844. [PubMed: 22743772]

Spinelli KJ, Taylor JK, Osterberg VR, Churchill MJ, Pollock E, Moore C, Meshul CK, Unni VK. Presynaptic alpha-synuclein aggregation in a mouse model of Parkinson's disease. J Neurosci. 2014 Feb 5; 34(6):2037–2050. PubMed PMID: 24501346; PubMed Central PMCID: PMC3913861. [PubMed: 24501346]

Styren SD, Hamilton RL, Styren GC, Klunk WE. X-34, a fluorescent derivative of Congo red: a novel histochemical stain for Alzheimer's disease pathology. J Histochem Cytochem. 2000 Sep; 48(9): 1223–1232. PubMed PMID: 10950879. [PubMed: 10950879]

Tanaka M, Kim YM, Lee G, Junn E, Iwatsubo T, Mouradian MM. Aggresomes formed by alpha-synuclein and synphilin-1 are cytoprotective. J Biol Chem. 2004 Feb 6; 279(6):4625–4631. Epub 2003 Nov 19. PubMed PMID: 14627698. [PubMed: 14627698]

Unni VK, Weissman TA, Rockenstein E, Masliah E, McLean PJ, Hyman BT. In vivo imaging of alphasynuclein in mouse cortex demonstrates stable expression and differential subcellular compartment mobility. PLoS One. 2010 May 11.5(5):e10589. PubMed PMID: 20485674; PubMed Central PMCID: PMC2868057. [PubMed: 20485674]

Volpicelli-Daley LA, Luk KC, Patel TP, Tanik SA, Riddle DM, Stieber A, Meaney DF, Trojanowski JQ, Lee VM. Exogenous α-synuclein fibrils induce Lewy body pathology leading to synaptic dysfunction and neuron death. Neuron. 2011 Oct 6; 72(1):57–71. PubMed PMID: 21982369; PubMed Central PMCID: PMC3204802. [PubMed: 21982369]

Wakabayashi K, Tanji K, Odagiri S, Miki Y, Mori F, Takahashi H. The Lewy body in Parkinson's disease and related neurodegenerative disorders. Mol Neurobiol. 2013 Apr; 47(2):495–508. Epub 2012 May 24. Review. PubMed PMID: 22622968. [PubMed: 22622968]

Waxman EA, Giasson BI. Specificity and regulation of casein kinase-mediated phosphorylation of alphasynuclein. J Neuropathol Exp Neurol. 2008 May; 67(5):402–416. PubMed PMID: 18451726; PubMed Central PMCID: PMC2930078. [PubMed: 18451726]

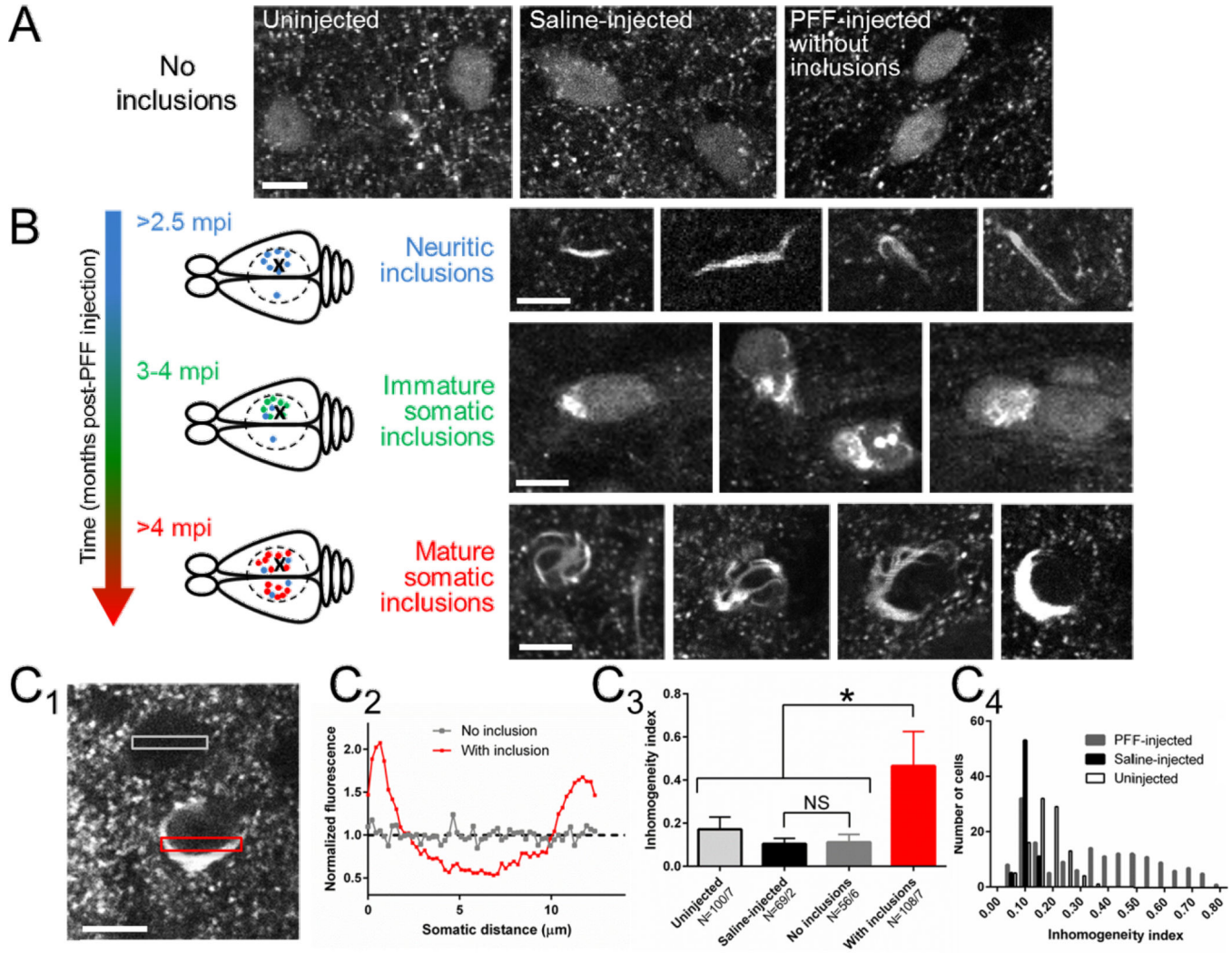

Figure 1. *In vivo* imaging demonstrates a stage-like, progressive maturation of Syn-GFP inclusions within neurons

A) *In vivo* imaging in cortex layer II/III of uninjected (left), saline-injected (middle) or PFF-injected (right) animals at 2 mpi demonstrates punctate presynaptic staining within the neuropil and only homogenous somatic Syn-GFP staining within neurons. Scale bar 10 μm. (B) Top: Starting at 2.5 mpi, imaging near the PFF injection site demonstrates frequent neuritic Syn-GFP aggregates in layer II/III, and rare neuritic aggregates in the contralateral hemisphere in the symmetric location to the injection. Schematic representation shows injection location in the right hemisphere (X), extent of cranial window (dashed circle), and location of neuritic aggregates (blue dot). Scale bar 10 μm. Middle: At 3–4 mpi, neurons (green dot in schematic) near the injection site began showing neurons with both disorganized somatic Syn-GFP inclusions and normal homogenous staining. Scale bar 10 μm. Bottom: At 4–13 mpi only mature, organized somatic and neuritic Syn-GFP inclusions are present. Mature somatic inclusions have a stereotyped appearance, often with a single juxtanuclear accumulation and legs that wrap around the nucleus, giving a “spider-like” appearance. The normal homogenous somatic and nuclear Syn-GFP staining is absent in

neurons containing mature inclusions. Schematic representation shows location of numerous mature somatic inclusions (red dot) near the injection site and in the contralateral hemisphere. Scale bar 10 μm.

(C) Example of two neurons (C_1), one with normal homogeneous staining and one with a mature inclusion, and transect ROIs used to measure fluorescence (C_2) across the cell body. An inhomogeneity index was calculated (see Methods) and used to measure the mean index value (C_3) in neurons from uninjected, saline-injected, and PFF-injected animals with and without inclusions. Neurons from uninjected, saline-injected and PFF-injected animals without inclusions show low levels of inhomogeneity, while inclusion-bearing neurons from PFF-injected animals were significantly more inhomogeneous. N = cells/animals. Histogram of inhomogeneity index values from cells from all three groups (C_4) shows single populations with low inhomogeneity in uninjected and saline-injected animals, while PFF-injected animals show two distinct populations, a low index one nearly identical to saline-injected animals, and a high index population corresponding to neurons with mature somatic inclusions. Scale bar 10 μm.

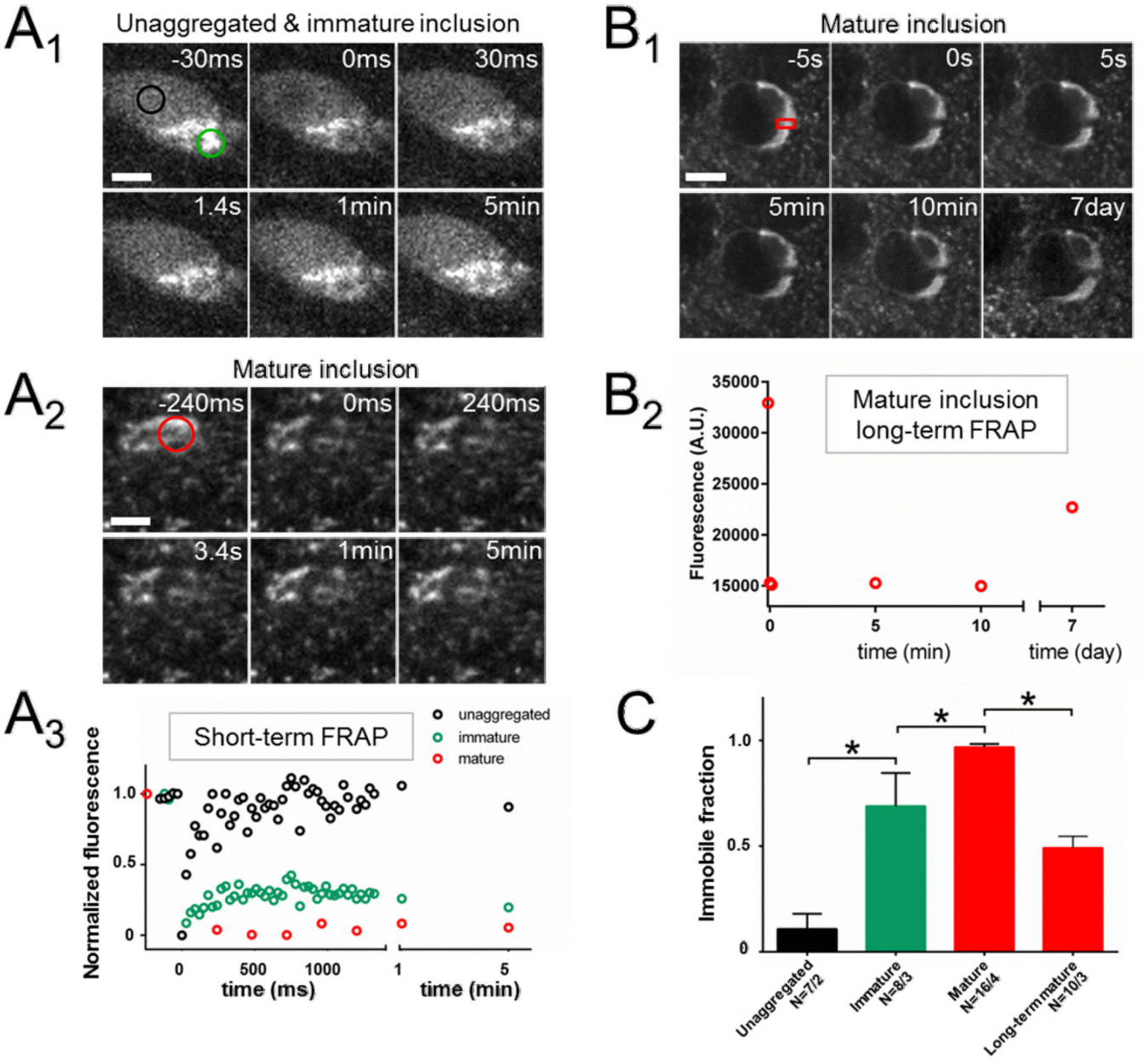

Figure 2. ***In vivo*** **FRAP demonstrates progressive compaction of and a low molecular turnover rate within Syn-GFP inclusions**

(A) Individual neuron (A_1) with an immature inclusion at 3 mpi demonstrates mixed aggregated and unaggregated somatic Syn-GFP staining pattern. Two ROIs, one within (green circle) and one outside (black circle) the aggregated portion are photobleached simultaneously and sequential images shown before and after FRAP. Bleach pulse occurs just before time 0. Scale bar 5 μm. Similar FRAP experiment of the aggregated portion (red circle) of a mature inclusion (A_2) at >4 mpi. Scale bar 5 μm. Mean fluorescence intensity (A_3) from the three ROIs from the two cells in $A_{1–2}$ plotted on the same time scale demonstrates complete recovery back to baseline of the homogeneous staining, but large immobile fractions in the immature and mature inclusions.

(B) Individual neuron (B_1) with a mature somatic inclusion at 4 mpi and absent unaggregated Syn-GFP staining in the remaining cytoplasm or nucleus. ROI (red rectangle) shows part of inclusion that was photobleached. Scale bar 7 μm. Mean intensity from this ROI over time (B_2) shows a large immobile fraction at 5–10 min post-bleach, which recovers substantially at 7 days post-bleach.

(C) Group data comparing measured immobile fractions from unaggregated somatic Syn-GFP, immature and mature inclusions at 5 min post-bleach, and mature inclusions 7 days post-bleach, showing a significant progressive increase in the immobile fraction from immature to mature inclusions as measured at 5 min. At 7 days post-bleach, however, 49% of the previously immobile fraction recovers, demonstrating a slow turnover of protein within inclusions. N = cells/animals.

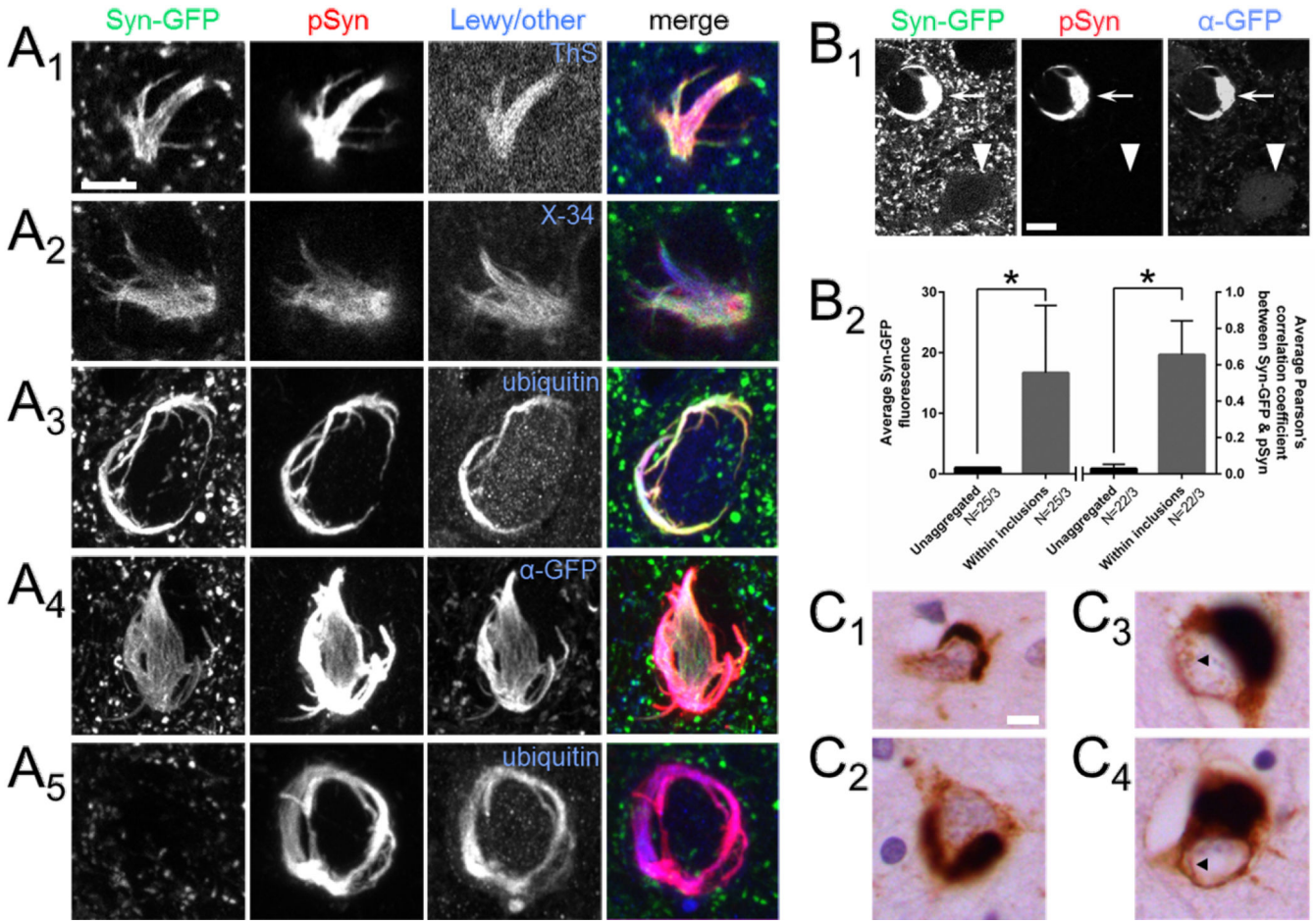

Figure 3. Mature somatic inclusions bear the hallmarks of human Lewy pathology

Mature Syn-GFP inclusions are heavily phosphorylated at serine-129 ($A_{1–4}$), in an amyloid dye binding configuration ($A_{1–2}$) and ubiquitinated (A_3). The green fluorescence from these inclusions is due to the presence of Syn-GFP and not an endogenous autofluorescent species, since they colabel with antibody to GFP (A_4). Similar mature inclusions made only of untagged endogenous mouse alpha-synuclein (A_5) are also present in nearby neurons that do not express Syn-GFP. These inclusions share a similar morphology and modification state to Syn-GFP-positive ones. Syn-GFP levels within mature inclusions (B, arrow) are greatly increased over levels of the protein in nearby neurons without inclusions (arrowhead). Colocalization of Syn-GFP with serine-129 phosphorylated alpha-synuclein (B) is also increased in inclusions versus cells without inclusions. N = cells/animals. Individual neurons from human frontal cortex in cases of Dementia with Lewy Bodies (C) are stained with hematoxylin to outline the nuclei in blue and for serine-129 phospho-synuclein aggregates in brown. Two examples demonstrate wrapping of aggregated alpha-synuclein around the nucleus ($C_{1–2}$), similar to that seen in mature mouse inclusions. Two other examples show “legs” of the inclusion that wrap around the nucleus ($C_{3–4}$, black arrowhead), also similar to mature mouse inclusions. Scale bar 5 μm. See also Fig. S1&2.

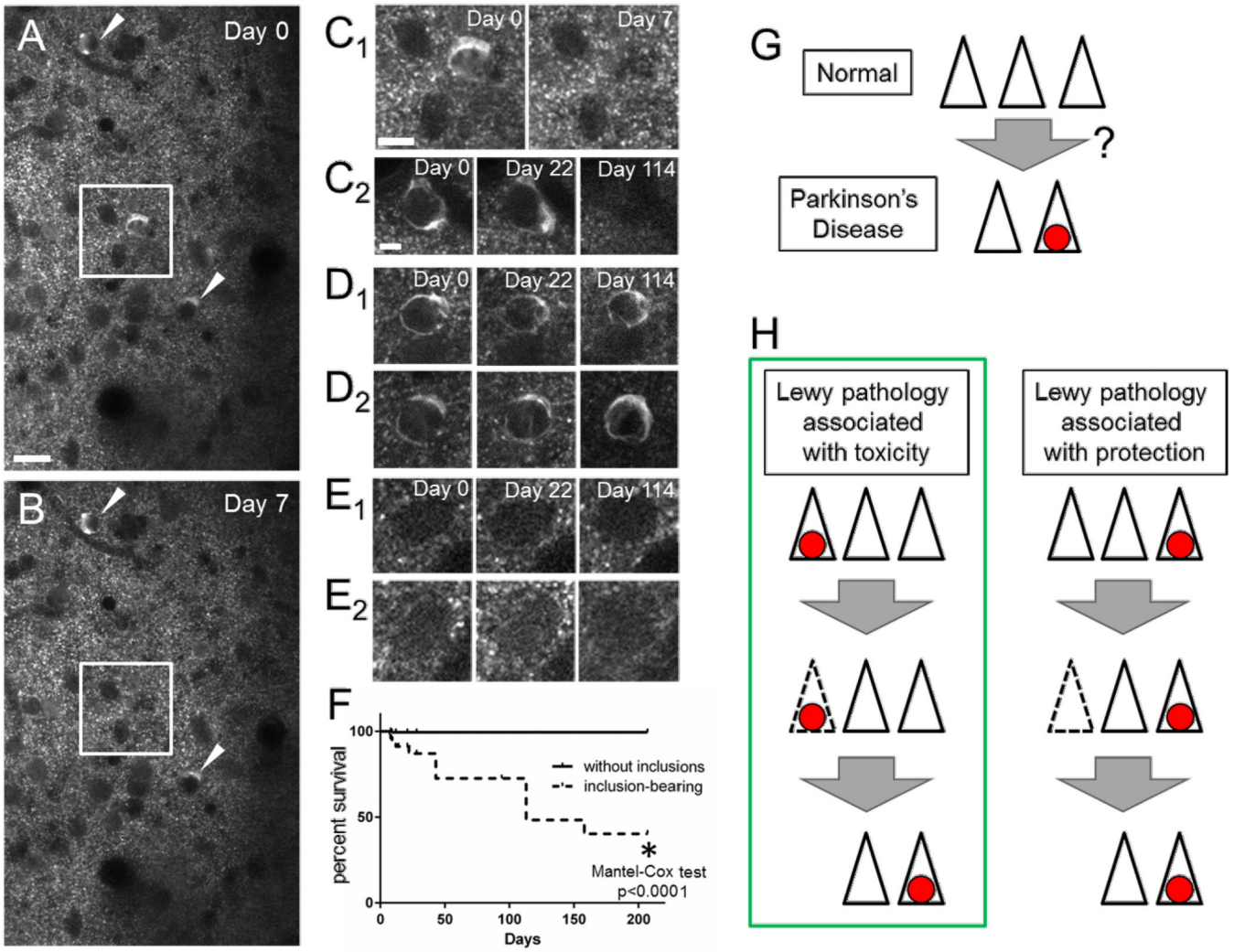

Figure 4. Chronic *in vivo* imaging demonstrates selective degeneration of inclusion-bearing neurons

Field of neurons (A&B) imaged one week apart demonstrate blood vessels by their negative stain, multiple neurons without inclusions and three mature inclusion-bearing neurons (white square & arrowhead) on Day 0. Scale bar 20 μm. One of these neurons (white square) degenerates by Day 7 and is shown at higher power (C_1). Scale bar C_1 10 μm, C_2-E_2 5 μm. Chronic imaging of individual neurons over months shows degeneration of some inclusion-bearing cells (C) with persistence of other cells with (D) and without (E) inclusions. Group data (F) shows selective degeneration of inclusion-bearing neurons over 7 months. Schematic showing the loss of neurons in brain regions affected by Parkinson's Disease with the presence of Lewy pathology (red circle) in some of the remaining cells (G), and two different models for how this same final state might arise (H). One model posits a positive correlation between Lewy pathology presence and cell death, while the other an inverse correlation.